STRUCTURAL GROUP ANALYSIS OF CORTICAL CURVATURE AND DEPTH PATTERNS IN THE DEVELOPING BRAIN

G. Operto[1] *G. Auzias*[2] *A. Le Troter*[2] *M. Perrot*[1] *D. Rivière*[1] *J. Dubois*[3] *P. Hüppi*[4] *O. Coulon*[2] *J-F Mang*

[1] LNAO, NeuroSpin, CEA, I2BM, Gif-sur-Yvette, France,
[2] LSIS Laboratory, CNRS UMR 6168, Marseille, France,
[3] U992 Cognitive NeuroImaging Unit, Gif-sur-Yvette, France,
[4] Geneva University Hospitals, Department of Pediatrics, Geneva, Switzerland

ABSTRACT

In the context of the study of brain morphogenesis, we present here a framework for surface-based group analysis using local cortical features in the neonate brain. We propose to detect and match local maxima from curvature and depth profiles of sulcal fundi. Such entities could have a key role to understand the variability of the brain morphology. We also describe a cortical localization tool dedicated to the developing brain. The proposed method is performed on a dataset of 25 preterm newborns and has detected consistent entities at the group level, both from cortical curvature and depth maps.

Index Terms— developing brain – cortical folding – intersubject variability – structural analysis

1. INTRODUCTION

The morphology of the cerebral cortex is highly complex and variable across individuals. In the past cortical folds have been studied conjointly with functional areas, connectivity and clinical data [1] and raised a renewal of interest as predictors of underlying cytoarchitecture [2] or pathologies [3]. Nevertheless the architectural organization of the cortex and the gyrification process are still poorly understood. Besides, imaging the developing brain has lately opened the possibility to follow the ontogenesis of the folding patterns step by step [4] and to study the brain at a stage where the intersubject variability is emerging [5].

This motivates the search for stable elementary units [6] or deep sulcal landmarks [7] modeling the cortex topography. However, very few methods extend this search to the developing brain where the folding patterns are still appearing. For instance existing works describe the sulcation process either by computing displacement fields on meshes [8], using spatiotemporal atlases [9], longitudinal registration [10] or by statistical analysis of region-based folding descriptors [11, 12]. In this work, we adapted a surface-based graph matching technique to extract from cortical curvature and depth maps sets of local maxima with spatial stability and groupwise reproducibility. We demonstrate its efficiency on a database of 25 preterm newborns of various gestational ages. We present results for two primary folds *i.e.* the Central (CS) and Superior Temporal Sulci (STS), both among the first to appear during sulcogenesis. We then define an anatomically-informed cortex-based referential adapted to the developing brain, which we use to evaluate the spatial distribution of these detected maxima.

2. MATERIALS AND METHODS

2.1. Data Preparation

For both hemispheres, gray and white matter are segmented and inner cortical surfaces are meshed from the T2-weighted images (mean number of vertices: 3700 +/- 1000) using tools from BrainVisa [4]. Mean curvature and depth maps are estimated from each mesh. Gaussian scale-spaces [13] are consecutively computed by iteratively smoothing each map along the mesh in order to track local maxima with cross-scale stability and get rid of noise. These maxima are then merged across scale levels following a simple geodesic distance criterion. The latter is estimated with respect to the spatial distribution of maxima in each subject independently in order to fusion close ones considered as same objects, while preserving relevant objects apart from one another. Merged maxima are then considered as individual candidates *i.e.* as inputs in the analysis described below.

2.2. Structural Group Analysis

Group analysis is performed using an object-based graph matching method adapted from [13]. In [13], intersubject matching is achieved using cortex-based coordinates. In this present method subjects are nonlinearly registered in 3D space using SPM8 [14]. A group graph $\mathcal{G}$ is initially built as follows : individual candidates, *i.e.* merged maxima, from each of the N_S subjects are taken as nodes $\{s\}$ and edges $\{c\} = C_{sim}$ are set between nodes if they belong to distinct subjects and are close enough ($< 10mm$) in the reference

space. A label field X is then optimized over the graph, relying on a detection model with rules on measure values (*e.g.* curvature or depth), stability in scale-space, relative positions and intersubject reproducibility. In the optimal realization of X, nodes carrying the same positive label identify the same group structure (zero is the non-interest class). By modeling X as a Markov Random Field, its best configuration is obtained by minimizing the sum of four energy terms :

$$U(X|Y) = \sum_{s\in\mathcal{G}} V_d(y_s|x_s) + \sum_{s\in\mathcal{G}} V_e(x_s) + \sum_{c\in C_{sim}} V_{sim}(c) + \sum_{\substack{i\in[\![1,N_S]\!]\\ \mathcal{G}_i\subset\mathcal{G}}} V_{ps}(\mathcal{G}_i) \quad (1)$$

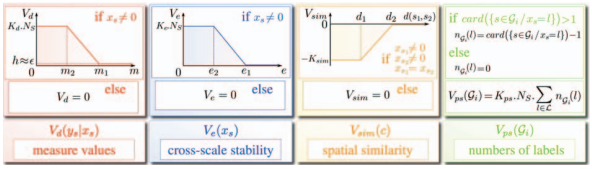


Fig. 1. Potentials of the energy : $[m_1, m_2]$ (resp. $[e_1, e_2]$ and $[d_1, d_2]$) is an interval defined on the value of the measure of interest (curvature or depth) (resp. cross-scale lifetime e and intersubject distance d). These parameters were tuned empirically except m_1 and m_2, defined from the data real distribution. $K_{\{\}}$ denominates the weights associated to the various potentials: with K_d=0.4, $K_e = 0.2$, $K_{sim} = 1.0$, $K_{ps} = 4.0$, we choose to give higher influence to spatial intersubject context than to measures. At this early stage of development, some folding areas may have low curvature/depth which is compensated by group-level information.

with Y being the input data, x_s the label carried by node s, y_s the data associated to s. V_d and V_e encourage, respectively, maxima with high measures (curvature or depth) and those with high scale-space lifetime, to carry positive labels. V_{sim} favors the detection of pairs of maxima with low Euclidean distance and V_{ps} penalizes every label l (among a set $\mathcal{L}$ of possible labels) appearing more than once in the same subject's subgraph $\mathcal{G}_i$ (Fig. 1). Minimization of the energy function is achieved by Gibbs sampling with simulated annealing. The analysis results in distinct sets of maxima with positive labels. The model promotes any label covering the whole group of N_S subjects but still concedes the creation of subgroups.

2.3. Anatomically-Informed Surface-Based Cortical Referential for the Developing Brain

Spatial normalization is often discussed over its effect on subsequent intersubject analyses [15], especially regarding cortical structures. In the foregoing, spatial normalization is performed using 3D nonlinear normalization which is suitable with the low folding degree in the premature brain. However, evaluating the spatial distribution of the local maxima using a different common space is a way to measure results

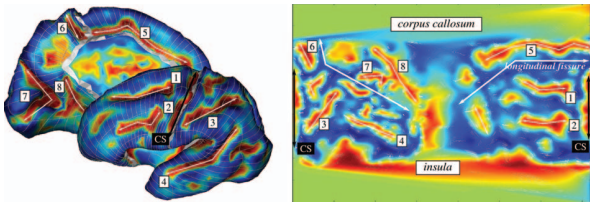


Fig. 2. *(left)* Surface-based referential defined on the developing cortical surface – *(right)* Flat map of the same cortical surface with numbered sulci superimposed

robustness. In this context, a cortical referential dedicated to the developing anatomy was implemented using a coordinate diffusion process adapted from [16]. A first step consists in manual segmentation over each hemisphere mesh of the *insula* and the *corpus callosum* area using a new interactive landmark editor developed in the BrainVisa/Anatomist package[17]. Both structures are assigned with specific values (0 for the corpus callosum, 180 for the insula) in the system as being the two poles of a latitudes/longitudes referential. The CS and the STS are also delineated. A longitude and a latitude maps are then computed by solving a constrained heat equation over the mesh, as in [16]. In those maps, the CS has always the same longitude and the STS, insular and cingular poles, have always the same latitude, thus defining an intersubject matching. Every mesh node therefore gets assigned with a latitude/longitude couple. This subsequently allows to build flat maps of the neonatal cortex.

3. RESULTS

The intrasubject spatial distribution of local maxima was estimated during the merging step by varying the distance criterion, named δ, and counting the number of maxima n_m after merging, in the CS and STS regions on curvature and depth maps (Fig. 3). In each case, n_m's standard deviation across subjects exhibits an initial rapid fall ($\delta < 4mm$) followed by a slower decay to finally reach convergence ($\delta > 16mm$; mean $\bar{n_m} = 1$ deviation $\sigma = 0$) when all maxima have fusioned in one single cluster. With respect to this, we retain $\delta = 4mm$ as a reasonable distance parameter for the merge.

Structural group analysis was performed both on cortical curvature and depth maps, left and right hemispheres (Fig. 4 and 5). Curvature analysis reveals a set of 4 maxima found in most subjects both along the CS and the STS in both hemispheres (Fig. 4). Depth analysis results in two sets of stable maxima along the CS and the STS. A third label is also carried by a subgroup of subjects in the posterior part of the STS (Fig. 4 *in purple, last row*).

Intersubject spatial distribution of the labeled curvature maxima for the CS was assessed (Fig. 5) using both the 3D nonlinear reference space and surface-based referential (section 2.3). The different clusters are associated to quite specific

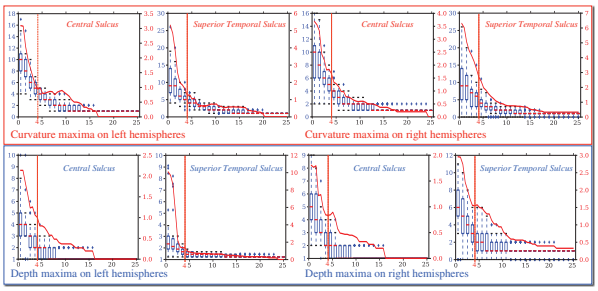


Fig. 3. Spatial distribution of maxima: number of maxima n_m across subjects *(blue boxplots, left y axis)* for various values of the distance criterion δ *(x axis)*. Standard deviation of this number across subjects is shown as a red curve *(right y axis)*.

local domains. These tend to slightly overlap, due to the remaining intersubject variability even after normalization.

4. DISCUSSION

In the context of brain development, sulci first appear as small grooves on the cortical surface : one of these can hence be identified as an emerging sulcus if frequently observed across subjects. With respect to this, structural analysis is able to overcome intersubject variability by jointly relying on individual and group-level information. In particular, such a model might shift the labels in one subject with regard to the others as long as it can improve group-level global consistency, even when better local pairwise matching might be found. Moreover, in contrast with other approaches, such an analysis provides results directly on each subject's anatomy and makes no use of any average template which is bound to smooth off individual features. Accessing results on individual representations is indeed of essential interest when dealing with anatomical questions.

The two depth maxima detected in the CS region are consistent with previous observations in adults [18, 7] and may be related to sulcal 'roots' [19, 8]. Two maxima are detected in each subject along the STS (three in a subset of subjects) : in this case, both the emerging state of this sulcus and the poor estimation of depth in this area might underestimate the number of identifiable units. On this matter, future work will investigate the correlation between number of units and gestational age. Four units were detected by curvature analysis, in each hemisphere, both in the CS and the STS regions. Joint analysis with diffusion-weighted data would help to compare these *e.g.* using connectivity-based parcellations. Curvature and depth maps contain information of different natures which explains the differences in group analysis results in numbers and positions of detected units (Fig. 4) : curvature globally embeds more details on the surface local geometry and is more sensitive, especially on the sulcal walls, than depth which rather describes the existence of pits [7].

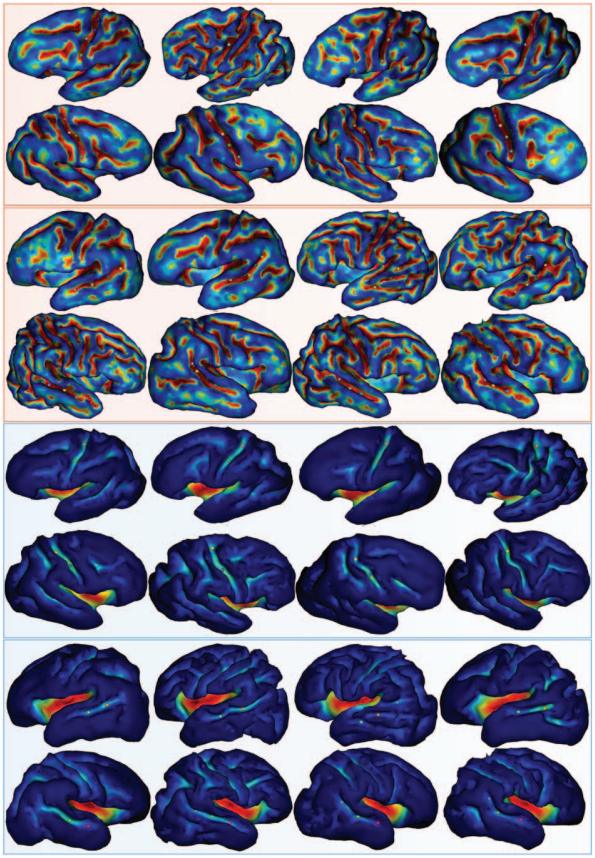


Fig. 4. Detected maxima for the cortical curvature *(top)* and depth *(bottom)* along the Central Sulcus *(rows 1,3)* and the Superior Temporal Sulcus *(rows 2,4)* on both hemispheres: each sphere color corresponds to a label. Four subjects among the most illustrative cases are shown for each series of images.

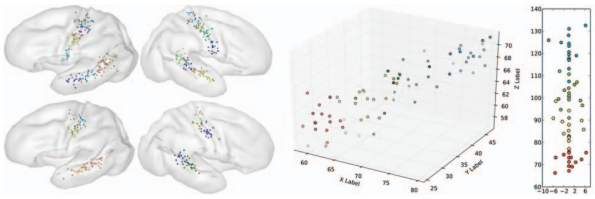


Fig. 5. *(left)* Group results of the curvature analysis *(top)* and depth analysis *(bottom)* presented on a template surface: each color corresponds to a label (in depth analysis only the two most reproducible labels are represented) – *(right)* Dispersion plots of detected curvature maxima along the left CS in 3D and 2D referentials

Finally, comparing the spatial distribution of the detected curvature maxima between volume and surface-based referentials highlights specific local domains associated with the maxima in both systems (Fig. 5). The dispersion in 3D space implies that the analysis overcame intersubject variability successfully. On the other hand, these same labeled entities show consistent localization on a cortical referential defined by anatomical markers, suggesting that they are spatially stable along the CS anatomical axis and that this stability is not a side effect of the sole iconic normalization process. This referential in its current version is actually a starting point towards an iterative extension of the structural analysis to other cortical regions using anatomical coordinates.

5. CONCLUSIONS

In this paper, we adapted the framework of structural analysis, originally proposed for fMRI data [13], to the search for common elementary units in developing brains. In comparison to existing works, this graph matching method aims at retrieving objects with cross-subject jittering positions, directly over each anatomy. Besides, we implemented a cortical localization tool for the developing brain embedding user-defined constraints along emerging landmarks. Surface-based approaches are still new to early brain development and such a framework suggest new insights on how cortical morphogenesis may be addressed.

Curvature and depth analyses of data covering most stages of sulcogenesis hence suggest the existence of stable entities possibly associated to meaningful landmarks of the cortex topography. Their interpretation remains to be linked to other concepts *e.g.* sulcal roots, pits, growth seeds [7, 8, 19] as well as to underlying connectivity. Future work will expand structural analysis to the study of longitudinal changes and will assess the relevance of new constraints in the cortical referential in order to find entities across the entire surface.

6. REFERENCES

[1] JF. Mangin et al., "In-vivo measurement of cortical morphology: means and meanings," *Curr Opin Neurol*, vol. 23–4, pp. 359–67, 2010.

[2] B. Fischl et al., "Cortical folding patterns and predicting cytoarchitecture," *Cereb Cort*, vol. 18–8, pp. 1973–80, 2008.

[3] H. Kim et al., "Basal temporal sulcal morphology in healthy controls and patients with temporal lobe epilepsy," *Neurology*, vol. 70–22, pp. 2159–65, 2008.

[4] J. Dubois et al., "Mapping the early cortical folding process in the preterm newborn brain," *Cereb Cort*, vol. 18–6, pp. 1444–54, 2008.

[5] T. White et al., "The development of gyrification in childhood and adolescence," *Brain Cogn*, vol. 72–1, pp. 36–45, 2010.

[6] A. Cachia et al., "A primal sketch of the cortex mean curvature: a morphogenesis based approach to study the variability of the folding patterns," *IEEE Trans Med Imag*, vol. 22–6, pp. 754–765, 2003.

[7] K. Im et al., "Spatial distribution of deep sulcal landmarks and hemispherical asymmetry on the cortical surface," *Cereb Cort*, vol. 20–3, pp. 602–11, 2010.

[8] J. Lefèvre et al., "Identification of growth seeds in the neonate brain through surfacic Helmholtz decomposition," *IPMI*, vol. 21, pp. 252–63, 2009.

[9] V. Rajagopalan et al., "Local Tissue Growth Patterns Underlying Normal Fetal Human Brain Gyrification Quantified In Utero," *J Neurosci*, vol. 31–8, pp. 2878–2887, 2011.

[10] H. Xue et al., "Longitudinal cortical registration for developing neonates," *MICCAI*, vol. 10, pp. 127–35, 2007.

[11] R. Pienaar et al., "A methodology for analyzing curvature in the developing brain from preterm to adult," *IJIST*, vol. 18–1, pp. 42–68, 2008.

[12] SP. Awate et al., "Cerebral cortical folding analysis with multivariate modeling and testing: Studies on gender differences and neonatal development," *NeuroImage*, vol. 53–2, pp. 450–459, 2010.

[13] G. Operto et al., "Surface-based structural group analysis of fMRI data," 2008, vol. 11, pp. 959–66.

[14] J. Dubois et al., "Structural asymmetries of perisylvian regions in the preterm newborn," *NeuroImage*, vol. 52–1, pp. 32–42, 2010.

[15] U. Yoon et al., "The effect of template choice on morphometric analysis of pediatric brain data," *NeuroImage*, vol. 45–3, pp. 769–77, 2009.

[16] C. Clouchoux et al., "Model-driven parameterization of the cortical surface for localization and inter-subject matching," *NeuroImage*, vol. 50–2, pp. 552–66, 2010.

[17] A. Le Troter et al., "An interactive sulcal fundi editor in BrainVisa," *OHBM*, 2011.

[18] MD. Cykowski et al., "The central sulcus: an observer-independent characterization of sulcal landmarks and depth asymmetry," *Cereb Cortex*, vol. 18–9, pp. 1999–2009, 2008.

[19] J. Régis et al., "Sulcal Root Generic Model: a Hypothesis to Overcome the Variability of the Human Cortex Folding Patterns," *Neurol Med Chir*, vol. 45, pp. 1–17, 2004.